1-1-2013

The effects of FEC (fluoroethylene carbonate) electrolyte additive on the lithium storage properties of NiO (nickel oxide) nanocuboids

Kuok H. Seng
University of Wollongong, kseng@uow.edu.au

Li Li
University of Wollongong, li@uow.edu.au

Dapeng Chen
University of Wollongong, dapeng@uow.edu.au

Zhixin Chen
University of Wollongong, zchen@uow.edu.au

Xiaolin Wang
University of Wollongong, xiaolin@uow.edu.au

See next page for additional authors

The effects of FEC (fluoroethylene carbonate) electrolyte additive on the lithium storage properties of NiO (nickel oxide) nanocuboids

Abstract

Nanocuboid shaped NiO (nickel oxide) has been synthesized using an optical floating zone furnace. It was found that the nanocuboids exhibit single crystalline nature, and have clean and sharp edges. Furthermore, the NiO nanocuboids were tested for their electrochemical performances as anode material for LIBs (lithium-ion batteries) in a coin-type half cell. The effects of FEC (fluoroethylene carbonate) additive on the lithium storage performance were also investigated, which is the first of such studies for transition metal oxides. It was found that FEC has a positive effect on the cycling stability and also improves the rate performances of the nanocuboids. The capacity recorded at 0.1C (100mAg-1) after 50 charge/dischargecycles is 1400mAhg-1. Lastly, the NiO nanocuboids can achieve very high rate capability of 12C (12Ag-1) with capacity of 312mAhg-1. 2013 Elsevier Ltd.

Keywords

electrolyte, effects, carbonate, oxide, fluoroethylene, fec, properties, storage, nio, lithium, nickel, additive, nanocuboids

Disciplines

Engineering | Physical Sciences and Mathematics

Publication Details

Seng, K. H., Li, L., Chen, D., Chen, Z., Wang, X., Liu, H. K. & Guo, Z. (2013). The effects of FEC (fluoroethylene carbonate) electrolyte additive on the lithium storage properties of NiO (nickel oxide) nanocuboids. Energy, 58 (September), 707-713.

Authors

Kuok H. Seng, Li Li, Dapeng Chen, Zhixin Chen, Xiaolin Wang, Hua-Kun Liu, and Zaiping Guo

The Effects of Fluoroethylene Carbonate Electrolyte Additive on the Lithium Storage Properties of Nickel Oxide Nanocuboids

Kuok Hau Seng,[ab] Li Li,[a] Da-Peng Chen,[a]* Zhi Xin Chen,[b] Xiao-Lin Wang,[a] Hua Kun Liu,[a] and Zai Ping Guo[ab]*

[a] Institute for Superconducting and Electronic Materials, University of Wollongong, NSW 2500, Australia

[b] School of Mechanical, Materials and Mechatronics Engineering, University of Wollongong, NSW 2522, Australia

E-mail: zguo@uow.edu.au (Z. P. Guo); dapeng@uow.edu.au (D. P. Chen)

Website: http://isem.uow.edu.au

Keywords: lithium battery, nanocube, nickel oxide, single crystal, vapor-solid

Abstract

Nanocuboid shaped nickel oxide has been synthesized using an optical floating zone furnace. It was found that the nanocuboids exhibit single crystalline nature, and have clean and sharp edges. Furthermore, the nickel oxide nanocuboids were tested for their electrochemical performances as anode material for lithium-ion batteries in a coin type half-cell. The effects of fluoroethylene carbonate additive on the lithium storage performance were also investigated, which is the first of such studies for transition metal oxides. It was found that fluoroethylene carbonate has a positive effect on the cycling stability and also improves the rate performances of the nanocuboids. The capacity recorded at 0.1 C (100 mA g^{-1}) after 50 charge/discharge cycles is 1400 mAh g^{-1}. Lastly, the nickel oxide nanocuboids can achieve very high rate capability of 12 C (12 A g^{-1}) with capacity of 312 mAh g^{-1}.

Introduction

Lithium-ion batteries (LIBs) have attracted considerable research interest since their introduction in the early 1990s. [1] This is mainly due to the higher energy density compared to other competing battery systems such as nickel-metal hydrides and nickel-cadmium batteries. Recently, mobile devices and electric vehicles have become the largest applications for LIBs. Although the demand for higher power and higher energy density storage systems has been constantly increasing, advances in LIBs have been relatively slow. This is because most LIBs on the market today still use the traditional electrode materials, which are graphite and $LiCoO_2$. Research on the different aspects of battery systems, such as management systems and modelling of battery usage, have been carried out to improve the performance. [2-7] However, new electrode materials replacing the current commercial materials are needed to improve both the power and the energy density of LIBs. Transition metal oxides are attractive alternatives to graphite as anode materials for LIBs due to their ability to react up to 8 mol Li-ions per formula unit. The 3*d* transition metal oxides have been extensively studied since the discovery of highly reversible lithium storage in transition metal oxide nanoparticles by Poizot *et al.* in 2000. [8] Among them, nickel oxide (NiO) is one of the most promising candidates, due to its higher theoretical gravimetric and volumetric capacities (720 mAh g^{-1}; 4800 mAh cm^{-3}) compared to graphite (372 mAh g^{-1}; 820 mAh cm^{-3}). In addition, nanostructured morphologies of transition metal oxides could affect the electrochemical lithium storage properties. Nickel oxides with different morphologies such as nanoparticles, [9] nanofibers, [10] nanotubes, [11] nanowalls, [12] nanoshafts, [13, 14] nanocones, [15] nanoflakes, [16-18] nanostructure hierarchical spheres, [19] and mesoporous structures [20] have been previously studied. In addition, nickel oxide composites with different carbon structures such as carbon coatings, [21, 22] carbon nanotubes, [10, 23] conducting polymers, [24, 25] and graphene [26-28] have also been reported. There have not been any studies on

cubic-shaped NiO nanostructures and their lithium storage properties, although NiO has a cubic rock salt structure. Furthermore, electrolyte additives have been studied for LIBs in order to improve the cycle life and safety of the cells. Organic additives such as vinylene carbonate (VC) [29-32] and fluoroethylene carbonate (FEC) [33-35] are the two most studied additives in regards to graphite and silicon anode materials. Both these electrolyte additives are known to form solid electrolyte interphase (SEI) layers of different compositions when added to conventional carbonate based electrolytes. Several reports in literature have shown that electrolytes containing FEC improve the cycling stability of silicon-based anode materials. Surprisingly, there has been little study on the effects of FEC additive on transition metal oxide performances.

In this work, we used an optical floating zone furnace to synthesize cubic-shaped NiO nanocrystals. This novel synthesis method has been reported in our recent publication. [36] This technique has been used for the crystal growth of a wide range of materials including both congruently and incongruently melting materials, however, the growth of nanomaterials using such approach have been rarely reported. The main advantage of this method is that no crucible is necessary, thus avoiding contaminants from the crucible. Furthermore, the temperature can be adjusted from room temperature to 2000°C with a controlled heating area of down to 3 millimetres on the target. This would give rise to a sharp temperature gradient (about 300°C cm^{-1}), which is beneficial in nanocrystal synthesis. This growth process is governed by the vapor-solid reaction mechanism. Due to the unique features and simplicity, we envisage that this method could be extended to synthesize other metal oxide nanocrystals. The as-prepared NiO were tested for their lithium storage properties. The possible reasons for the excellent electrochemical properties in relation to the FEC additive are discussed in this work.

Experimental Methods

The nickel oxide nanocuboids were synthesized using an infrared radiation furnace equipped with four 300 W tungsten halogen lamps (JIH 100V-300WC-CS) as previously reported by our group. [36] A schematic diagram of the furnace set-up and the reaction mechanism is presented in Fig. 1. In a typical experiment, NiO powder (99.8%) was pressed to form a rod shaped target 6 mm in diameter and 30 mm in length. The NiO target was further sintered at 1150°C overnight in air. Then, the NiO target was loaded onto the rotating sample holder and the system was sealed and evacuated to remove air. The target was then adjusted vertically so that the tip was in line with the central heating zone. Oxygen gas (99%) was introduced into the furnace so as to flow vertically upwards at 100 mL $minute^{-1}$. Next, the light beams from the lamps were focused on the tip of the target to start the evaporation process. The temperature was then increased to 1600°C within 6 min, and the target was rotated at a speed of 20 rpm. The system was left to run for 48 hours, and the grey-green product was collected from the walls of the quartz tube. The synthesis was repeated three times and in each batch, about 0.5 g of sample was collected.

The as-synthesized samples were characterized using X-ray diffraction (GBC MMA), field emission scanning electron microscopy (JOEL JSM7500), and transmission electron microscopy (JOEL 2010). For the electrochemical tests, the nickel oxide nanocuboids were mixed with conductive carbon (Super-P), polyacrylic acid (Sigma Aldrich) and carboxy methyl cellulose (Sigma Aldrich) in a ratio of 70:15:7.5:7.5. Water was added to the mixture to form uniform slurry, which was then coated on copper foil using a doctor blade. The electrode was then dried at 150°C under vacuum for 2 hours. Round disks 9.5 mm in diameter were punched from the dried electrode, and the loading of active material (NiO) in each electrode was 0.9 ± 0.1 mg cm^{-2}. 2032-type coin cells were assembled in an argon-filled

glove box using the punched disk electrodes, lithium metal as the counter electrode, and a polypropylene separator (Cellgard). The electrolytes used were 1 M $LiPF_6$ in ethylene carbonate/dimethyl carbonate/diethyl carbonate (EC/DMC/DEC; 3/4/3 v/v; Novolyte) and 1 M $LiPF_6$ in EC/DMC/DEC (3/4/3 v/v; Novolyte) with 5 wt% fluoroethylene carbonate (FEC) additive. As the cells were tested as half-cells, the term "discharge" is related to the lithium insertion into the NiO, and the term "charge" is related to lithium extraction from the NiO. The cells were tested on a Land Battery Cycler for galvanostatic charge/discharge performance, and cyclic voltammetry tests were performed on a Bio-Logic VMP3 electrochemical workstation. For each electrochemical characterization, the tests were repeated at least 4 times.

Results and Discussions

The as-prepared NiO cuboid nanocrystals were first characterized using X-ray diffraction (XRD), and a typical pattern is presented in Fig. 2(a). There are five distinct peaks which can be indexed to cubic NiO (ICDD #47-1049). In addition, there are no other peaks present in the XRD pattern, indicating that there is no impurity phase detectable in the sample. Then, the morphology of the as-prepared nanocuboids was investigated using scanning electron microscopy (SEM), and the micrographs are presented in Fig. 2(b) and (c). It should be noted that a thin layer of platinum (~3 nm) was coated on the surface of the nanocuboids for SEM imaging. From the SEM images, the NiO nanocrystals have a cuboid shape with sharp edges and flat surfaces. The sizes of the nanocrystals were determined to be in the range of 10 to 80 nm. Transmission electron microscopy (TEM) was performed to further study the morphology of the samples. In Fig. 2(d), nanocuboids can be observed with sizes of about 20 nm that are resting on the carbon replica. Upon closer inspection, the nanocuboids have clean edges and appear to be single crystalline (Fig. 2(e)). The fast Fourier transformed (FFT) diffraction pattern of the corresponding image is shown in the inset, indicating the single crystallinity. The bright dots can be indexed to the (200) plane of cubic NiO. Under high resolution TEM mode, the lattice spacing of the NiO nanocuboids can be observed, as shown in Fig. 2(f), which is the magnified area indicated by the white arrow in Fig. 2(e). The *d*-spacing was measured to be 0.208 nm, corresponding to the (200) plane of NiO, which is in agreement with the FFT diffraction pattern.

The as prepared NiO nanocuboids were then tested for their lithium storage properties in coin-type half cells with lithium as the counter electrode. Electrolytes with and without additives were used in this study to investigate the optimal lithium storage performance. In order to understand the electrochemical reactions of the NiO nanocubes, cyclic voltammetry was performed on the assembled coin cells at a scan rate of 0.1 mV s^{-1}. The cyclic

voltammetry (CV) curves for the cells both with and without electrolyte additive are presented in Fig. 3. In should be noted that the CV profiles both with and without FEC appear similar, which signifies that the lithium reaction mechanism is not altered by the electrolyte additive. During the first reduction scan, a sharp peak can be observed at 0.3 V, which corresponds to the electrochemical reduction of the NiO to Ni and Li_2O. In the first oxidation scan, the small hump centered at 1.5 V and the peak at 2.25 V can be related to the re-oxidation of Ni to NiO. At the second reduction scan, the peak indicating lithium reaction with NiO has shifted to 1.1 V. In the corresponding oxidation scan, the peaks at 1.5 V and 2.25 V appear to have increased in current density. This is consistent with the galvanostatic cycling results, which showed increased capacity with cycling. In the 6^{th} CV cycle, both the redox peaks show increased specific current density, which further confirms the capacity increase effect.

For the cycling stability tests, all the cells were charge/discharged at 0.05 C (1 C = 1 A g^{-1}) for the initial 2 cycles, then at 0.1 C, 1 C, or 4 C (Fig. 3(c) and (d)). The initial coulombic efficiency recorded for all the cells was 66%, regardless of the electrolyte additive, which is normal for transition metal oxide anode materials. The loss in capacity is due to the decomposition of electrolyte to form the solid electrolyte interphase (SEI) layer. When, the cells were tested without FEC at 0.1 C (Fig. 3(c)), the discharge capacity recorded was 1040 mAh g^{-1} at the 3^{rd} cycle, and the capacity increased to 1170 mAh g^{-1} at the 26^{th} cycle. Then, the capacity remained relatively stable up to the 35^{th} cycle, where the capacity was 1055 mAh g^{-1}. In the subsequent cycles, however, a sharp drop in capacity was observed, and the capacity recorded at the 50^{th} cycle was 495 mAh g^{-1}. The capacity loss can be attributed to the degradation of the NiO. It is well known that NiO undergoes a conversion reaction which features large volume changes during cycling. In addition, these volume changes would cause cracks, which form new SEI layers that will lower the conductivity of the electrode, and

cause isolation of metallic Ni and Li_2O, as well as pulverization of the electrode. Furthermore, evidence of degradation of the electrode and formation of new SEI layer can be seen from the Coulombic efficiency of the cell, as presented in Fig. 3(e). After 35 cycles, where the sharp drop in capacity occurs, the Coulombic efficiency drop from 98% to 92%, then the Coulombic efficiency became unstable. When cycled at 1 C, the capacity recorded at the 3rd cycle was 922 mAh g^{-1}, and the capacity gradually faded to 596 mAh g^{-1} over 50 cycles. At 4 C, the capacity recorded at the 3rd cycle was 662 mAh g^{-1}, and the capacity faded to 111 mAh g^{-1} at the 50th cycle. From these cycling results, it should be noted that the capacities recorded initially at rates of 0.1 C and 1 C are higher than the theoretical value of 720 mAh g^{-1}, for 2 Li^+ reaction per NiO. The extra capacity can be mainly attributed to the formation of a reversible polymer/gel layer on the surface of the active materials and the interfacial storage of lithium within the Ni/Li_2O matrix. Laruelle *et al.* reported on the formation of a conducting polymer/gel film from the decomposition of the electrolyte, which gives rise to pseudocapacitive behavior that increases the lithium storage. [37] In addition, Balaya *et al.* proposed that Li-ions were stored interfacially on the surfaces of the metallic nanoparticles through the charge separation mechanism at low potentials. [38]

On the other hand, when the NiO nanocuboid electrodes were tested using the electrolyte with 5 wt% FEC additive, the lithium storage performance was greatly enhanced (Fig. 3(d)). At 0.1 C, the initial capacity at the 3rd cycle was 1052 mAh g^{-1}. The electrode showed a similar trend towards capacity increase with cycling, recording 1400 mAh g^{-1} after 50 cycles. It should be noted that the recorded capacity is almost twice the theoretical capacity of NiO (720 mAh g^{-1}). Moreover, the Coulombic efficiency remained stable at 98% from the 2nd cycle to the 50th cycle (Fig. 3(e)). When cycled at the 1 C-rate, the capacity recorded at the 3rd cycle was 904 mAh g^{-1}, and very little capacity fading was observed, with a capacity of 864 mAh g^{-1} remained after 50 cycles. At 4 C, the capacity recorded at the 3rd cycle was 710 mAh

g^{-1} and at the 50th cycle, 557 mAh g^{-1} was retained. These results, to the best of our knowledge, are the best ever reported for NiO based anode material. Although the capacity at 0.1 C is almost twice the theoretical capacity, it is still lower than the first discharge capacity (1600 mAh g^{-1}). Therefore, the high capacity can be attributed to the reversible formation of SEI layer, and the interfacial lithium storage as discussed earlier. Fig. 4(a) and (b) shows the voltage profile and the dQ/dV, respectively, at the 2^{nd}, 25^{th} and 50^{th} cycle. Increment of the discharge capacities at the lower voltage regions can be seen with increased cycling. The discharge capacities recorded below 0.8 V are usually associated with SEI formation and interfacial lithium storage. Furthermore, the increase in surface area caused by the electrochemical milling effect also contributes toward the increase of reversible SEI formation and interfacial lithium storage. In order to further investigate the capacity increase phenomenon, ex-situ TEM analysis of the electrode materials were performed after the 1^{st} and the 50^{th} cycles at the fully charged state. The morphology of the NiO nanocuboids after the 1^{st} cycle is presented in Fig. 4(c). It should be noted that the general shape of the nanocuboids remained, however, upon closer inspection (insets of Fig. 4(c)), the single crystalline structure was destroyed. Small crystallites can be observed from the high resolution TEM image. This agrees well with the conversion reaction mechanism where NiO forms Ni and Li_2O during lithiation and, then forms NiO again after delithiation. The conversion reaction mechanism is also known to have an electrochemical milling effect, where bulk crystals can be reduced to nanosized crystallites after repeated cycling. [39] This effect can be clearly observed in the sample after 50 cycles, as shown in Fig. 4(d). The NiO nanocuboids had disintegrated and formed nanosized particles among the carbon black and binder. The inset of Fig. 4(d) shows the corresponding electron diffraction pattern where all the rings can be indexed to NiO and metallic Ni. Moreover, the reduction of the crystallite size of the active materials can also be interpreted as an activation process where more active

surface area for the lithium reaction is generated. Thus, the capacities were observed to increase with cycling. Similar phenomena have also been reported for other transition metal oxides. [40-43]

The NiO nanocuboids were further tested for rate performance and the results are shown in Fig. 5(a) and (b). The cells were tested for 6 cycles at each charge/discharge rate: 0.1 C, 1 C, 2 C, 4 C, 6 C, 8 C, 10 C, 12 C, 14 C, and 16 C. The voltage profiles plotted in Fig. 5(a) and (b) are those of the 6th cycle at every rate. When the electrolyte without FEC additive was used, the capacity recorded at 0.1 C, 1 C, 2 C, 4 C, and 6 C was 1056 mAh g^{-1}, 714 mAh g^{-1}, 570 mAh g^{-1}, 421 mAh g^{-1}, and 258 mAh g^{-1}, respectively. As the rate was increased further from 8 C to 16 C, the capacity decreased from 172 mAh g^{-1} to 80 mAh g^{-1}. The rate performance of NiO nanocuboids improved when FEC additive was used. The capacity recorded at 0.1 C, 1 C, 2 C, 4 C, and 6 C was 1060 mAh g^{-1}, 933 mAh g^{-1}, 884 mAh g^{-1}, 798 mAh g^{-1}, and 713 mAh g^{-1}, respectively. When the rate was increased to 8 C, 10 C, 12 C, 14 C, and 16 C, the capacity recorded was 600 mAh g^{-1}, 444 mAh g^{-1}, 312 mAh g^{-1}, 230 mAh g^{-1}, and 190 mAh g^{-1}, respectively. The capacity recorded at the 12 C rate was still 312 mAh g^{-1}, which is comparable to the theoretical capacity of graphite. From the voltage profiles of the rate tests, it can be observed that the polarization increases more rapidly with the charge/discharge rate for the cells without electrolyte additive. We attribute the improvement in rate performance by a simple addition of FEC to the electrolyte to the differences in SEI layer formation. Nakai and co-workers studied the SEI formed by different electrolytes on silicon based electrodes. [34] They found that ethylene carbonate electrolytes form SEI layers which are mainly made of lithium oxides and lithium alkoxides, and the thickness increases with cycling. In contrast, electrolytes containing FEC form very thin SEI layers consisting of lithium fluoride and polyethylene compounds. In order to justify this hypothesis, we used electrochemical impedance spectroscopy (EIS) to probe the resistivity of the cells after

cycling. Fig. 5(c) and (d) show the impedance spectra of the cells with and without FEC additive, respectively, after 6 CV cycles. The resistance values were obtained by simulation of the spectrum using the equivalent circuit shown in Fig. 5(e). The SEI film resistance (R_{SEI}) and charge transfer resistance (R_{ct}) of the cells without FEC additive (R_{SEI} = 19.8 Ω; R_{ct} = 88.2 Ω) were twice as high as the cells with FEC (R_{SEI} = 6.8 Ω; R_{ct} = 45.1 Ω). Therefore, these results indicate that FEC additive forms a SEI layer on the surface of NiO that has lower electric and charge transfer resistance, which improves the electrochemical performance, similar to the effects on Si based electrode. This finding is crucial as a strategy to improve the lithium storage performances of other transition metal oxide anode materials. Further study, however, is required to understand the electrolyte decomposition mechanism and the SEI film formed by FEC additive on the surface of NiO.

Conclusion

In summary, we have synthesized single crystalline NiO nanocuboids through a vapor-solid process using an optical floating zone furnace. The nanocuboids have smooth surfaces, sharp edges, high crystallinity, and are between 5 and 80 nm in size. We found that the single crystallinity of the nanocuboids was destroyed after going through a few charge/discharge cycles, which is due to the nature of the conversion reaction. Furthermore, the higher specific capacity compared to the theoretical capacity is due to the nanosized nature of the NiO and the ability of transition metal oxides to store lithium through interfacial charge separation and the formation of a reversible polymer/gel layer. However, further study is required to fully understand the reasons behind the extra capacity. Last but not least, we have shown that addition of a small amount of FEC to the electrolyte would help in improving the cycling stability, and most importantly, increasing the rate performance of the NiO nanocuboids. Both the synthesis method and the FEC additive into the electrolyte could be applied to other transition metal oxides.

Acknowledgement

This work is supported by an Australian Research Council (ARC) Discovery Project (Grant Number DP1094261). The authors acknowledge use of facilities within the UOW Electron Microscopy Centre. The authors would like to thank Dr. Tania Silver for critical reading of the manuscript and valuable remarks.

References

[1] Tarascon JM, Armand M. Issues and challenges facing rechargeable lithium batteries. Nature. 2001;414(6861):359-67.

[2] Amjad S, Rudramoorthy R, Neelakrishnan S, Varman KSR, Arjunan TV. Evaluation of energy requirements for all-electric range of plug-in hybrid electric two-wheeler. Energy. 2011;36(3):1623-9.

[3] Avril S, Arnaud G, Florentin A, Vinard M. Multi-objective optimization of batteries and hydrogen storage technologies for remote photovoltaic systems. Energy. 2010;35(12):5300-8.

[4] He HW, Zhang XW, Xiong R, Xu YL, Guo HQ. Online model-based estimation of state-of-charge and open-circuit voltage of lithium-ion batteries in electric vehicles. Energy. 2012;39(1):310-8.

[5] Sun FC, Hu XS, Zou Y, Li SG. Adaptive unscented Kalman filtering for state of charge estimation of a lithium-ion battery for electric vehicles. Energy. 2011;36(5):3531-40.

[6] Vynnycky M. Analysis of a model for the operation of a vanadium redox battery. Energy. 2011;36(4):2242-56.

[7] Weng GM, Su YZ, Liu ZQ, Zhang JH, Dong W, Xu CW. Electrochemical properties of novel organodisulfide poly 1,2-bis(thiophen-3-ylmethyl)disulfane as cathode material for secondary lithium batteries. Energy. 2009;34(9):1351-4.

[8] Poizot P, Laruelle S, Grugeon S, Dupont L, Tarascon JM. Nano-sized transition-metaloxides as negative-electrode materials for lithium-ion batteries. Nature. 2000;407(6803):496-9.

[9] Huang XH, Tu JP, Zhang B, Zhang CQ, Li Y, Yuan YF, et al. Electrochemical properties of NiO-Ni nanocomposite as anode material for lithium ion batteries. Journal of Power Sources. 2006;161(1):541-4.

[10] Lu H-W, Li D, Sun K, Li Y-S, Fu Z-W. Carbon nanotube reinforced NiO fibers for rechargeable lithium batteries. Solid State Sciences. 2009;11(5):982-7.

[11] Needham SA, Wang GX, Liu HK. Synthesis of NiO nanotubes for use as negative electrodes in lithium ion batteries. Journal of Power Sources. 2006;159(1):254-7.

[12] Varghese B, Reddy MV, Yanwu Z, Lit CS, Hoong TC, Rao GVS, et al. Fabrication of NiO nanowall electrodes for high performance lithium ion battery. Chemistry of Materials. 2008;20(10):3360-7.

[13] Kavitha T, Yuvaraj H. A facile approach to the synthesis of high-quality NiO nanorods: electrochemical and antibacterial properties. Journal of Materials Chemistry. 2011;21(39):15686-91.

[14] Yuan L, Guo ZP, Konstantinov K, Munroe P, Liu HK. Spherical clusters of NiO nanoshafts for lithium-ion battery anodes. Electrochemical and Solid State Letters. 2006;9(11):A524-A8.

[15] Wang X, Yang Z, Sun X, Li X, Wang D, Wang P, et al. NiO nanocone array electrode with high capacity and rate capability for Li-ion batteries. Journal of Materials Chemistry. 2011;21(27):9988-90.

[16] Ci S, Zou J, Zeng G, Peng Q, Luo S, Wen Z. Improved electrochemical properties of single crystalline NiO nanoflakes for lithium storage and oxygen electroreduction. Rsc Advances. 2012;2(12):5185-92.

[17] Mai YJ, Tu JP, Xia XH, Gu CD, Wang XL. Co-doped NiO nanoflake arrays toward superior anode materials for lithium ion batteries. Journal of Power Sources. 2011;196(15):6388-93.

[18] Ni S, Li T, Yang X. Fabrication of NiO nanoflakes and its application in lithium ion battery. Materials Chemistry and Physics. 2012;132(2-3):1108-11.

[19] Liu L, Li Y, Yuan S, Ge M, Ren M, Sun C, et al. Nanosheet-Based NiO Microspheres: Controlled Solvothermal Synthesis and Lithium Storage Performances. Journal of Physical Chemistry C. 2010;114(1):251-5.

[20] Liu H, Wang G, Liu J, Qiao S, Ahn H. Highly ordered mesoporous NiO anode material for lithium ion batteries with an excellent electrochemical performance. Journal of Materials Chemistry. 2011;21(9):3046-52.

[21] NuLi Y, Zhang P, Guo Z, Wexler D, Liu H, Yang J, et al. Nanostructured NiO/C Composite for Lithium-Ion Battery Anode. Journal of Nanoscience and Nanotechnology. 2009;9(3):1951-5.

[22] Xia Y, Zhang W, Xiao Z, Huang H, Zeng H, Chen X, et al. Biotemplated fabrication of hierarchically porous NiO/C composite from lotus pollen grains for lithium-ion batteries. Journal of Materials Chemistry. 2012;22(18):9209-15.

[23] Xu C, Sun J, Gao L. Large scale synthesis of nickel oxide/multiwalled carbon nanotube composites by direct thermal decomposition and their lithium storage properties. Journal of Power Sources. 2011;196(11):5138-42.

[24] Huang XH, Tu JP, Xia XH, Wang XL, Xiang JY. Nickel foam-supported porous NiO/polyaniline film as anode for lithium ion batteries. Electrochemistry Communications. 2008;10(9):1288-90.

[25] Idris NH, Wang J, Chou S, Zhong C, Rahman MM, Liu H. Effects of polypyrrole on the performance of nickel oxide anode materials for rechargeable lithium-ion batteries. Journal of Materials Research. 2011;26(7):860-6.

[26] Huang Y, Huang X-l, Lian J-s, Xu D, Wang L-m, Zhang X-b. Self-assembly of ultrathin porous NiO nanosheets/graphene hierarchical structure for high-capacity and high-rate lithium storage. Journal of Materials Chemistry. 2012;22(7):2844-7.

[27] Zhou G, Wang D-W, Yin L-C, Li N, Li F, Cheng H-M. Oxygen Bridges between NiO Nanosheets and Graphene for Improvement of Lithium Storage. Acs Nano. 2012;6(4):3214-23.

[28] Zou Y, Wang Y. NiO nanosheets grown on graphene nanosheets as superior anode materials for Li-ion batteries. Nanoscale. 2011;3(6):2615-20.

[29] Aurbach D, Gamolsky K, Markovsky B, Gofer Y, Schmidt M, Heider U. On the use of vinylene carbonate (VC) electrolyte solutions for Li-ion as an additive to batteries. Electrochimica Acta. 2002;47(9):1423-39.

[30] Chen L, Wang K, Xie X, Xie J. Effect of vinylene carbonate (VC) as electrolyte additive on electrochemical performance of Si film anode for lithium ion batteries. Journal of Power Sources. 2007;174(2):538-43.

[31] Ota H, Sakata Y, Inoue A, Yamaguchi S. Analysis of vinylene carbonate derived SEI layers on graphite anode. Journal of the Electrochemical Society. 2004;151(10):A1659-A69.

[32] Wang YX, Nakamura S, Tasaki K, Balbuena PB. Theoretical studies to understand surface chemistry on carbon anodes for lithium-ion batteries: How does vinylene carbonate play its role as an electrolyte additive? Journal of the American Chemical Society. 2002;124(16):4408-21.

[33] Etacheri V, Haik O, Goffer Y, Roberts GA, Stefan IC, Fasching R, et al. Effect of Fluoroethylene Carbonate (FEC) on the Performance and Surface Chemistry of Si-Nanowire Li-Ion Battery Anodes. Langmuir. 2012;28(1):965-76.

[34] Nakai H, Kubota T, Kita A, Kawashima A. Investigation of the Solid Electrolyte Interphase Formed by Fluoroethylene Carbonate on Si Electrodes. Journal of the Electrochemical Society. 2011;158(7):A798-A801.

[35] Profatilova IA, Kim S-S, Choi N-S. Enhanced thermal properties of the solid electrolyte interphase formed on graphite in an electrolyte with fluoroethylene carbonate. Electrochimica Acta. 2009;54(19):4445-50.

[36] Chen D-P, Wang X-L, Du Y, Ni S, Chen Z-B, Liao X. Growth Mechanism and Magnetic Properties of Highly Crystalline NiO Nanocubes and Nanorods Fabricated by Evaporation. Crystal Growth & Design. 2012;12(6):2842-9.

[37] Laruelle S, Grugeon S, Poizot P, Dolle M, Dupont L, Tarascon JM. On the origin of the extra electrochemical capacity displayed by MO/Li cells at low potential. Journal of the Electrochemical Society. 2002;149(5):A627-A34.

[38] Balaya P, Li H, Kienle L, Maier J. Fully reversible homogeneous and heterogeneous Li storage in RuO2 with high capacity. Advanced Functional Materials. 2003;13(8):621-5.

[39] Choi JW, McDonough J, Jeong S, Yoo JS, Chan CK, Cui Y. Stepwise Nanopore Evolution in One-Dimensional Nanostructures. Nano Letters. 2010;10(4):1409-13.

[40] Hassan MF, Guo Z, Chen Z, Liu H. alpha-Fe2O3 as an anode material with capacity rise and high rate capability for lithium-ion batteries. Materials Research Bulletin. 2011;46(6):858-64.

[41] Hassan MF, Rahman MM, Guo ZP, Chen ZX, Liu HK. Solvent-assisted molten salt process: A new route to synthesise alpha-Fe2O3/C nanocomposite and its electrochemical performance in lithium-ion batteries. Electrochimica Acta. 2010;55(17):5006-13.

[42] Li L, Guo Z, Du A, Liu H. Rapid microwave-assisted synthesis of Mn3O4-graphene nanocomposite and its lithium storage properties. Journal of Materials Chemistry. 2012;22(8):3600-5.

[43] Seng KH, Du GD, Li L, Chen ZX, Liu HK, Guo ZP. Facile synthesis of graphene-molybdenum dioxide and its lithium storage properties. Journal of Materials Chemistry. 2012;22(31):16072-7.

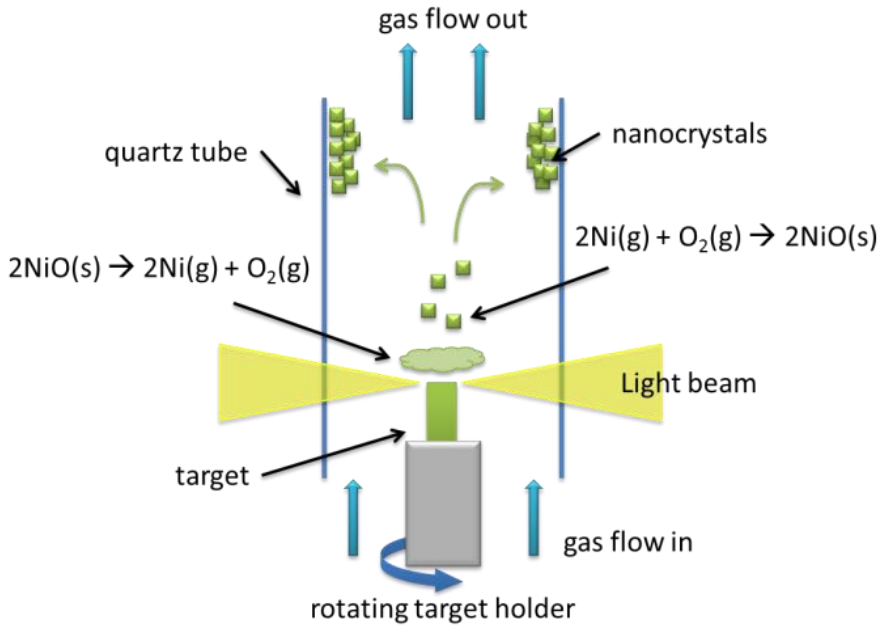

Fig. 1. Schematic diagram of the floating zone furnace with a tungsten based halogen lamp as the infrared radiation source. Carrier gas flows vertically upwards through the furnace at a controlled flow rate.

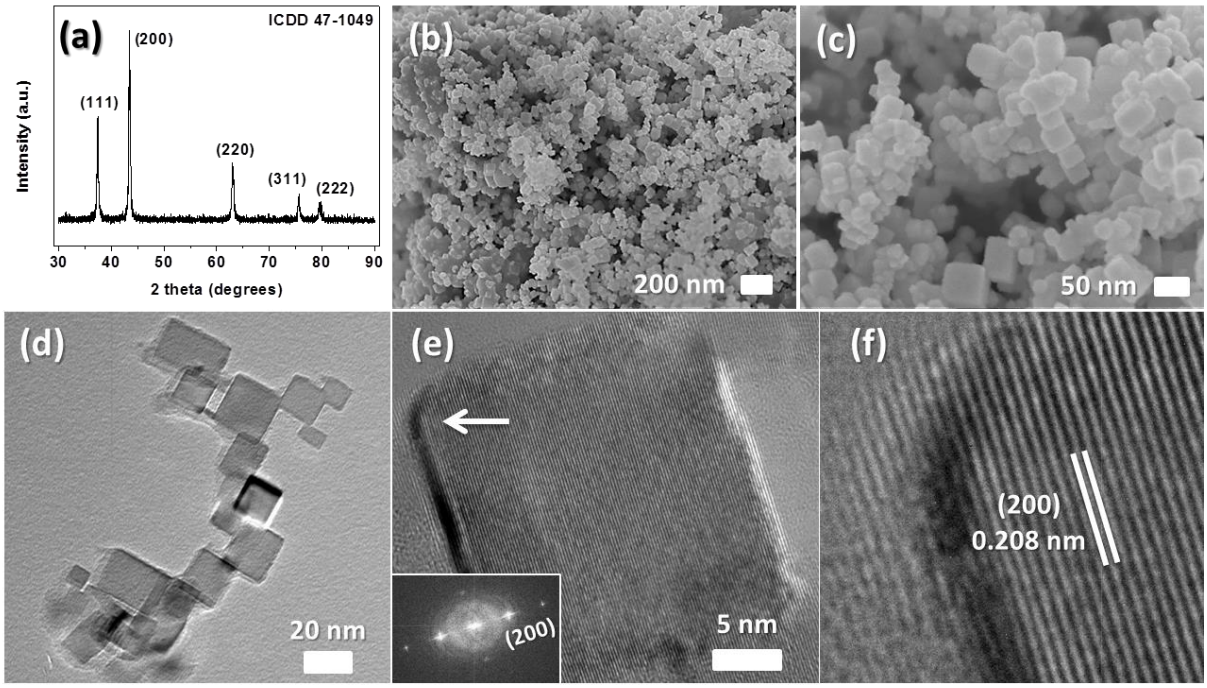

Fig. 2. (a) X-ray diffraction pattern of the as prepared NiO nanocuboids. All the diffraction peaks can be indexed to the cubic NiO phase (b,c) Scanning electron micrographs of the NiO nanocuboids. The size of the nanocuboids ranges from 5 to 80 nm. (d,e) Transmission electron micrographs of the as-preapred NiO showing the single crystalline nature of each cuboid; the inset shows the corresponding fast Fourier transform diffraction pattern of the corresponding nanocrystal (f) High resolution TEM image of the area marked by the white arrow in (e), showing the lattice spacing of the 200 planes.

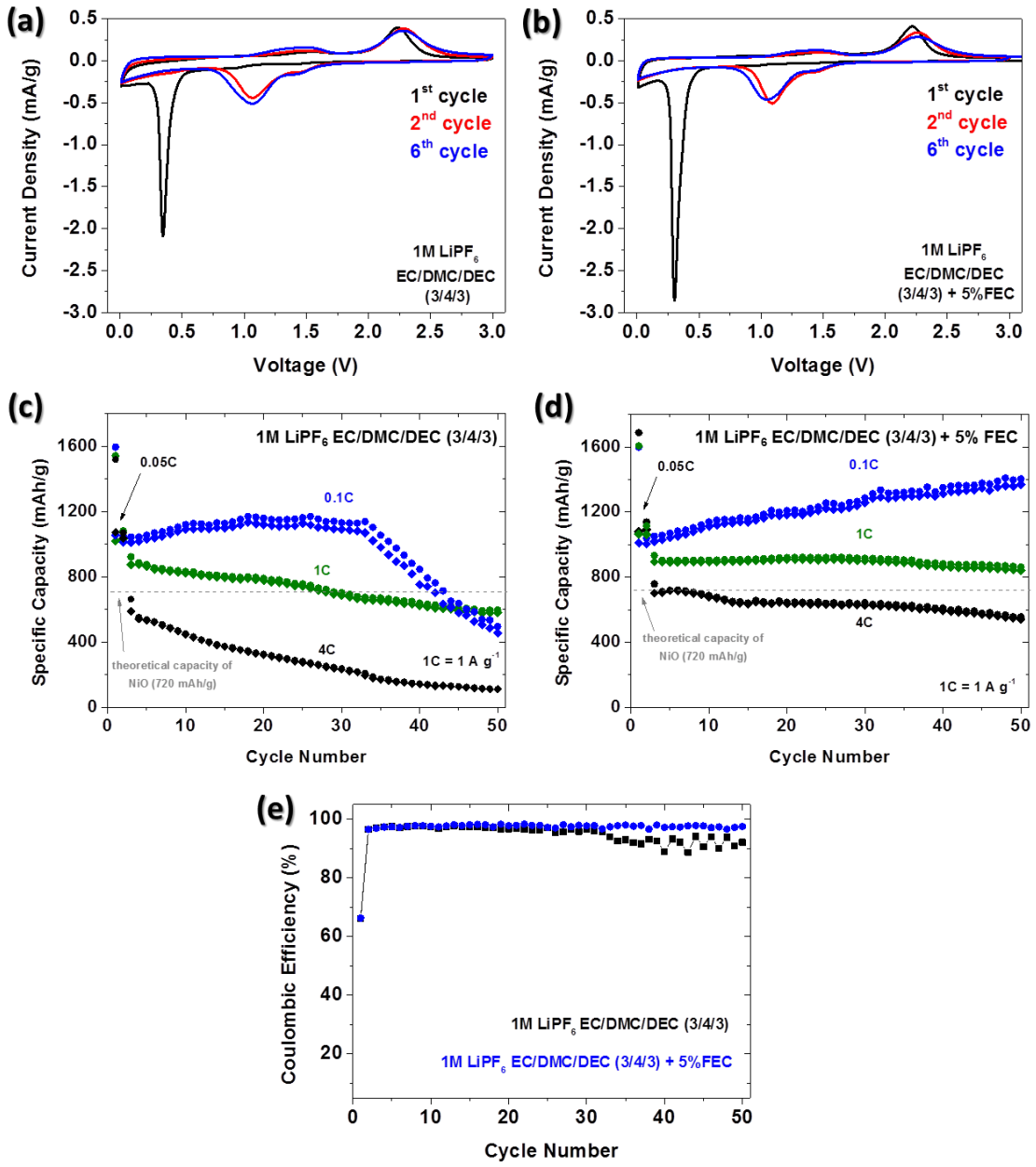

Fig. 3. Cyclic voltammograms for selected cycles of the NiO nanocuboid electrodes without (a) and with (b) 5 wt% FEC. Cycling performance of the NiO nanocuboid electrodes at 0.1C, 1C and 4C without (c) and with (d) 5 wt% fluoroethylene carbonate additive. (e) Coulombic efficiency of the cells charge/discharged at 0.1 C.

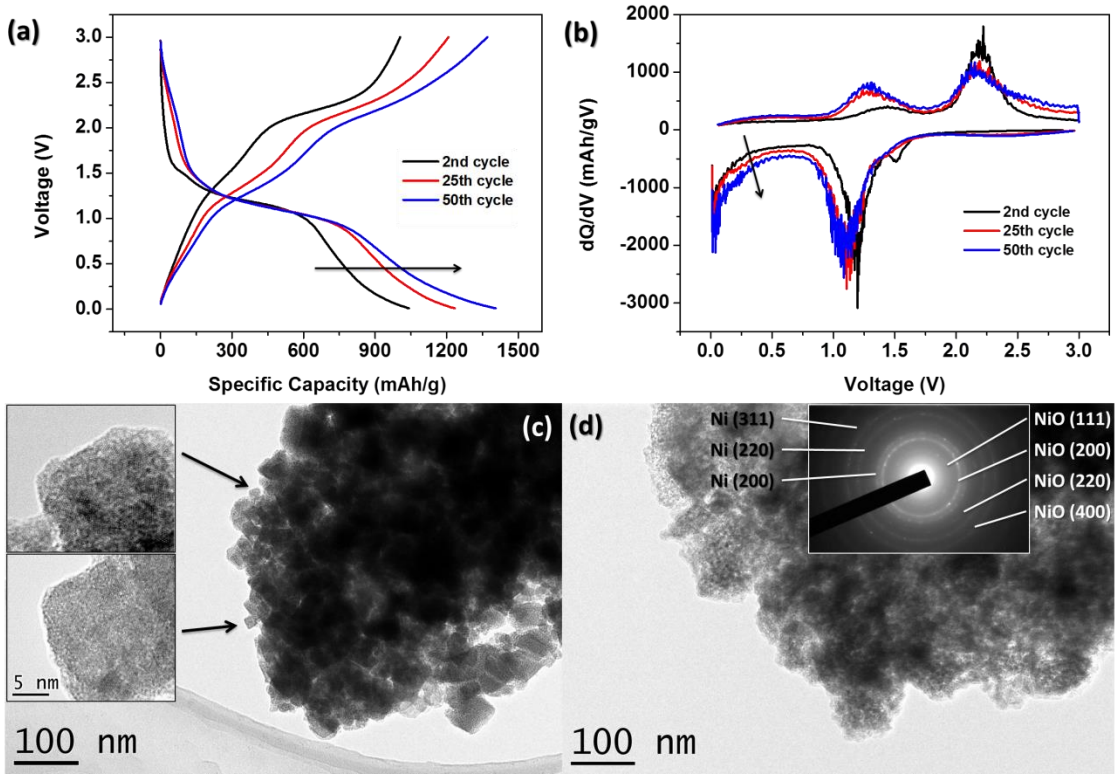

Fig. 4. (a) Voltage profile and (b) differential plots of NiO nanocuboids cycled at 0.1 C with 5 wt% FEC additive at the 2nd, 25th and 50th cycle. Transmission electron micrographs of the NiO nanocuboids (c) after 1 cycle. The insets are higher magnification images of the areas marked by the black arrows. The general shape of the nanocuboids was retained however, the single crystallinity was destroyed by the electrochemical lithium reaction. (d) After 50 cycles, the cuboid shape of the NiO has been destroyed. Higher magnification images could not be obtained due to the reactivity with the focused electron beam. The diffraction pattern in the inset can be indexed to the NiO and Ni phases.

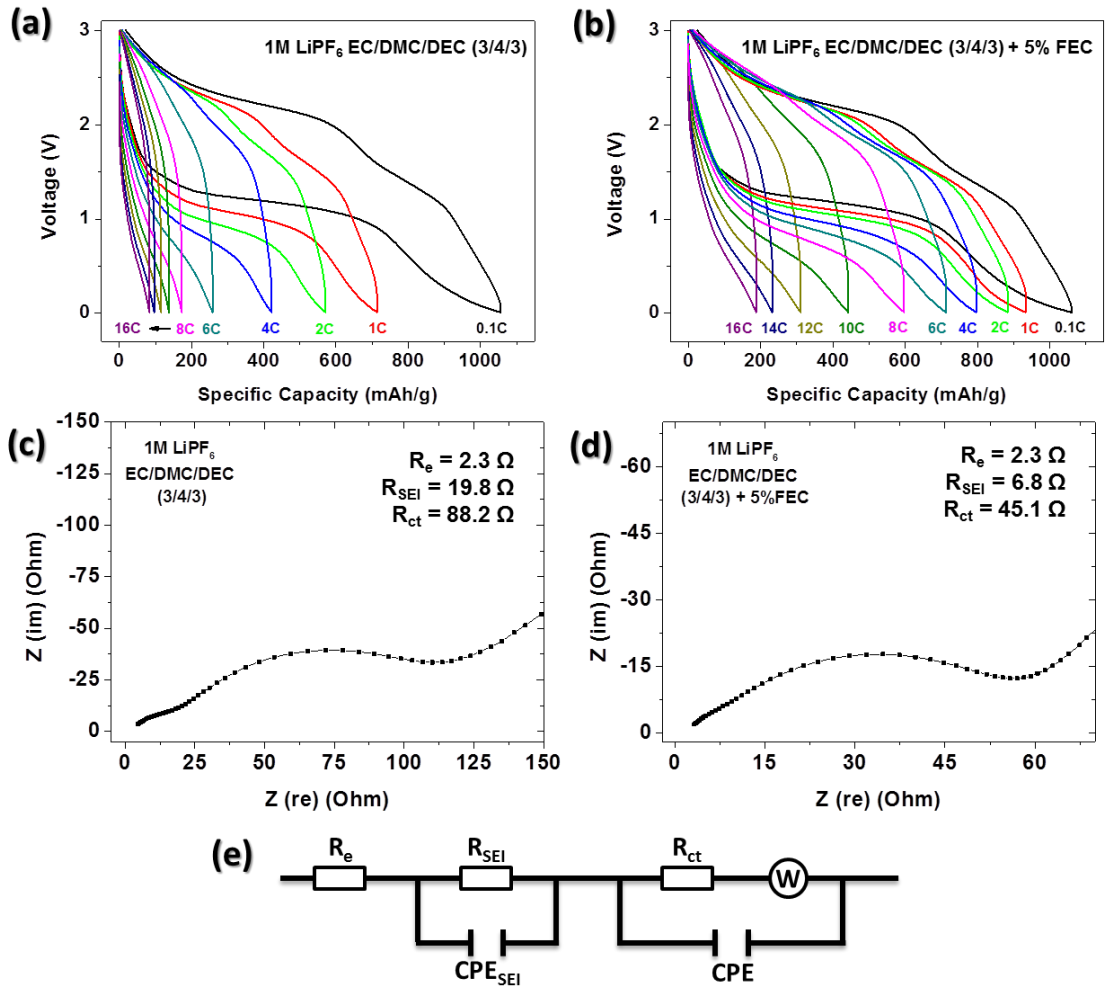

Fig. 5. Voltage profiles of the rate performances from 0.1 C to 16 C of NiO nanocuboid electrodes without (a) and with (b) 5 wt% fluoroethylene carbonate additive. The charge and discharge rates are equivalent. Electrochemical impedance spectra of NiO nanocuboid electrodes after 6 CV cycles without (c) and with (d) FEC additive; (e) the equivalent circuit used to simulate the resistivity of the electrodes.